AUT Journal of Modeling and Simulation

AUT J. Model. Simul., 57(2) (2025) 139-156
DOI: 10.22060/miscj.2025.24959.5443

Designing a new robust control method to reduce LFOs in the power system

Farhad Amiri*, Sajad Sadr

Department of Electrical Engineering, Tafresh University, Tafresh, Iran.

ABSTRACT: LFOs are among the most significant variables that lead to the loss of power system stability and the reduction of transmission line capacity. The SSSC is one of the parts used to increase the power system's stability. In this paper, in order to improve the stability of the power system and also to reduce the LFOs, the design of the SSSC equipped with a new robust controller is discussed, which is called output feedback based on LMI. The stability criterion of the suggested method is established based on the Lyapunov stability theory. The control objectives in the proposed method are the asymptotic stability of the system under the influence of disruption and parameter uncertainty as well as minimizing the impact of disturbance on the system states. SSSC equipped with output feedback method based on LMI with compensation based on RMPC methods, Fuzzy lead-lag optimized by PSO, Fuzzy lead-lag optimized by MWOA has been compared and the results are that the proposed method has a favorable performance compared to other control methods presented and has been able to withstand the uncertainty of parameters and disturbances. In order to compare the performance of the proposed method, simulations have been performed in different scenarios. The maximum deviations related to the rotor angular velocity are improved by 58% using the proposed method. The settling time related to rotor angular velocity deviations has been improved by 6% using the proposed method.

Review History:

Received: Oct. 22, 2025
Revised: Nov. 21, 2025
Accepted: Dec. 18, 2025
Available Online: Dec. 31, 2025

Keywords:

LFO
New Robust Controller
Lyapunov Stability Theory
SSSC

1- Introduction

FACTS devices are recognized as a new tool for power system management and control [1]. These devices are designed to increase the reliability, efficiency, and power transmission capacity in the power grid and play an important role in reducing power losses and increasing system stability [2]. These devices can be used for series and parallel compensation to maintain voltage and frequency under variable load conditions [3]. This is especially important in substations and transmission lines, because voltage and frequency fluctuations can damage equipment and reduce power quality. FACTS devices can increase transmission capacity [4]. These devices make power transmission more efficient by reducing leakage and increasing current efficiency [4]. FACTS devices optimize current and load, thereby reducing energy loss [5]. By accurately controlling reactive power and optimizing system efficiency, these devices can significantly reduce operating costs [6]. Another benefit of FACTS devices is the power system's stability, both dynamic and static. The system is more stable against alterations and disruptions because to this technology. FACTS devices are crucial to the grid's integration of renewable energy sources like solar and wind, which are growing in popularity [7]. These devices ensure that renewable sources are connected to the grid efficiently and continuously by controlling voltage and optimizing current. FACTS devices are also used in smart grids. Using these technologies, load management can be improved and energy demand can be predicted [8]. The classification of FACTS devices in terms of control type is of two types: 1) Thyristor-based FACTS device control 2) Voltage-source converter based on FACTS device control [9]. Power system stability is crucial, and dampening LFOs is one of the most crucial factors taken into account in power system stability [10]. As previously stated, LFOs in the power system can be dampened and suppressed by regulating the transmission line's reactive power. The SSSC is one of the most crucial FACTS devices for reducing LFOs in the power system [11]. SSSC is one of the key devices in the FACTS family. This gadget was created especially to regulate reactive power and enhance power systems' functionality. In order to properly manage voltage and current and lower LFOs in the power system, the SSSC injects or absorbs reactive power in series with the transmission lines [12]. The damping of LFOs of a power system using SSSC equipped with different controllers is studied in Table (1).

These methods are not robust against severe uncertainties related to the parameters related to the power system.

Consequently, a controller that is both resilient to the uncertainty of power system and disturbance-related parameters and lessens the impact of power system disturbances must be designed. This study presents a novel control strategy that relies on the system's feedback output.

*Corresponding author's email: f.amiri@tafreshu.ac.ir

Table 1. The damping of LFOs of a power system using SSSC equipped with different controllers.

SSSC equipped with various control methods	Advantages	Disadvantages
SSSC equipped with a PID controller [13,14]	This PID controller has a simple structure.	The PID controller does not perform well against uncertainties in power system parameters
SSSC equipped with a neuro-fuzzy controller [15]	This controller performs well against mild uncertainties	These controllers do not perform well against uncertainties and severe disturbances introduced into the system.
SSSC equipped with a neuro-fuzzy controller optimized with a multi-objective PSO [16]	This controller performs well against mild uncertainties	This control method does not perform well against severe disturbances and severe uncertainties
SSSC equipped with a PI controller optimized with a GA [17]	This PI controller has a simple structure	The PI controller does not perform well against disturbances and uncertainties related to power system parameters
SSSC controllers in power system using ant colony optimization algorithm [18]	This method performs well against mild uncertainties	This method is not effective against severe disturbances and uncertainties in power system parameters
SSSC equipped with an optimized POD controller using the MOA [19]	This method is resistant to disturbances.	This method is not robust against uncertainty in system parameters
SSSC equipped with an optimized FOPID controller using the GWO [20]	This method is suitable for mild uncertainty	This method is not effective against severe disturbances and uncertainties in power system parameters
SSSC fitted with a fuzzy controller [21, 22]	This controller performs well against mild uncertainties	These controllers do not perform well against uncertainties and severe disturbances introduced into the system.
SSSC fitted with a type 2 fuzzy controller [23]	This controller performs well against mild uncertainties	These controllers do not perform well against uncertainties and severe disturbances introduced into the system.
SSSC with a lead-lag controller tuned using MZOA [24]	This controller has a simple structure.	this approach is ineffective when dealing with extreme power system parameter uncertainty
SSSC equipped with a robust MPC [25]	This controller has a good performance against disturbances and uncertainties related to system parameters	However, to design this controller, it is necessary to convert the single-machine power system model from continuous space to discrete space, which causes problems such as sampling error, oscillations, and changes in stability
SSSC equipped with an optimal fuzzy lead-lag controller based on the MWOA [26]	This controller has a simple structure.	this approach is ineffective when dealing with extreme power system parameter uncertainty

The suggested approach just makes use of the feedback output and lacks the capability to measure every condition of the power system. There are two components to the suggested control system's goals: 1) The closed-loop system is asymptotically stable under parameter uncertainty in the absence of disturbance. 2) The closed-loop system with zero starting conditions achieves the performance $\frac{z_{L_2}}{w_{L_2}} \leq \gamma$ in the presence of disturbance and uncertainty.

The stability criterion of the proposed method is based on Lyapunov theory. First, the Lyapunov stability criterion for the linear system under study is obtained according to the power system space model. Then, using Schur complement theory and the lemmas mentioned in the article, the Lyapunov stability criterion has been transformed into the LMI. The LMIs have been solved in YALMAP, and by solving the LMI, the parameters of the proposed dynamic controller have been obtained. Also, the proposed controller has more degrees of freedom, which can be used to perform more effective control over the system, and there is no need to access the parameters of the closed-loop system to design the control system. In the following paper, first the said method is fully proven, then the said method is applied to a linear system (The designing of a SSSC to improve the stability of the power system) which also has uncertainty of parameters and disturbance, and the efficiency and effect of the proposed controller on the single-machine power system are compared with the optimal fuzzy lead-lag control based on the PSO, the optimal fuzzy lea-lag control based on MWOA, and the RMPC. The findings demonstrate that the suggested approach performs better than other suggested control strategies and can withstand disturbances and parameter ambiguity. There are several sections in the paper. The power system modeling is covered in the second section. In the third section, the design of the proposed method is discussed in order to improve the LFOs of the power system. In the fourth section, the simulation of the proposed method and its comparison with other control methods are discussed. In the fifth section, the conclusion is expressed.

2- Power System Modeling

2- 1- Connection of Static Series Compensation in Power System

Figure (1) shows the infinite bus single-machine power system considering SSSC. Table (2) shows the parameters related to the single-machine power system and the SSSC [20-25]. The small signal model of a single-machine power system connected to an infinite bus considering the proposed control for SSSC by the Heffron-Phillips model is shown in Figure (2) [.

The output voltage in the SSSC is controlled simultaneously with the control of the conduction time of the switches located in the voltage-source converter, and under any condition, by adjusting the voltage of the SSSC, the power of the transmission line is controlled. As shown in Figure (1), the power required in the SSSC is supplied through a capacitor located on the DC side of the converter. If the DC source has the necessary power to supply energy, the voltage injected into the line (V_{INV}) can be controlled in terms of angle and phase. Therefore, the SSSC can exchange active power and reactive power with the system. The size of the DC source is small if it is used only for the purpose of exchanging reactive power with the system (small capacitor).

The SSSC performs similarly to a controlled series reactor or capacitor because the injected voltage vector is perpendicular to the current and the voltage injected into the line can be 90 degrees ahead or behind the current. The series capacitor differs in that the voltage injected by the SSSC is independent of the line current, controllable, and effective under both low and high load situations. By producing capacitance and inductance voltages, the SSSC may adjust line power and establish advantageous circumstances for dampening power system-related LFOs. The wideband modulation approach is the foundation for the SSSC's functioning [20–25].

2- 2- Dynamic model of power system with SSSC

The power system oscillations have been analyzed using a small signal model. Equation (1) illustrates the small signal model of a single-machine power system coupled to

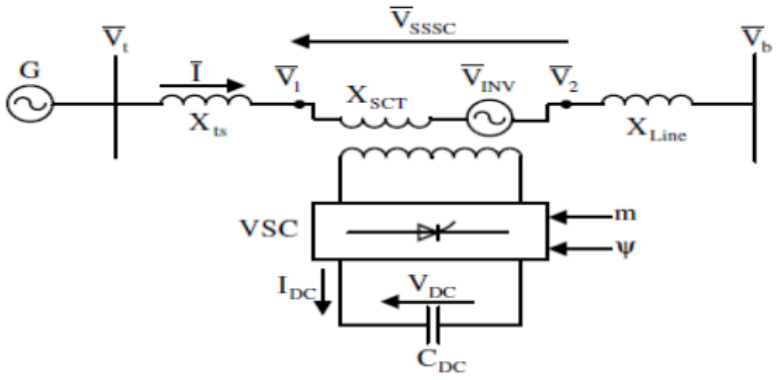

Fig. 1. The infinite bus single-machine power system considering SSSC [21, 22].

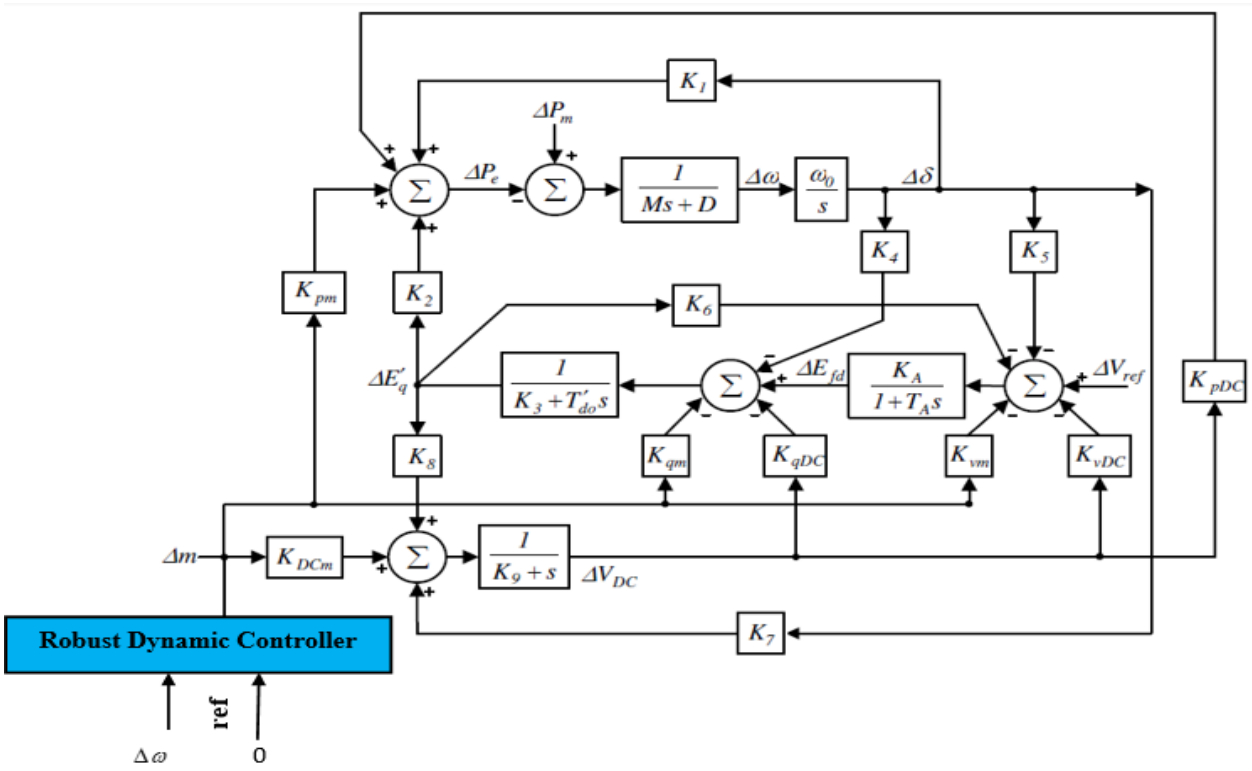

Fig. 2. The small signal model of a single-machine power system connected to an infinite bus considering the proposed control for SSSC [25].

an infinite bus, taking into account the SSSC controller via the Heffron-Phillips model. In equation (1), $\Delta\delta$: changes in the rotor angle of the synchronous generator, $\Delta\omega$: changes in the rotor angular velocity ($\frac{rad}{sec}$), ΔP_m: changes in the turbine output power, ΔP_e: changes in the generator power, M: inertia, D: damping factor, $\Delta E_q^{'}$: changes in the generator internal voltage, ΔE_{fd}: changes in the excitation winding voltage, Δm: signal generated by the proposed controller for SSSC, K_A: excitation winding gain, T_A: excitation winding time constant, and $T_{d0}^{'}$: open circuit time constant.

$$\begin{bmatrix}\dot{\Delta\delta}\\ \dot{\Delta\omega}\\ \dot{\Delta E_q^{'}}\\ \dot{\Delta E_{fd}}\\ \dot{\Delta V_{DC}}\end{bmatrix}=\begin{bmatrix}0 & \omega_0 & 0 & 0 & 0\\ \frac{-K_1}{M} & \frac{-D}{M} & \frac{-K_2}{M} & 0 & \frac{-K_{pDC}}{M}\\ \frac{-K_4}{T_{do}^{'}} & 0 & \frac{-K_3}{T_{do}^{'}} & \frac{1}{T_{do}^{'}} & \frac{-K_{dDC}}{T_{do}^{'}}\\ \frac{-K_A K_5}{T_A} & 0 & \frac{-K_A K_6}{T_A} & \frac{-1}{T_A} & \frac{-K_A K_{vDC}}{T_A}\\ K_7 & 0 & K_8 & 0 & -K_9\end{bmatrix}\begin{bmatrix}\Delta\delta\\ \Delta\omega\\ \Delta E_q^{'}\\ \Delta E_{fd}\\ \Delta V_{DC}\end{bmatrix}+\begin{bmatrix}0\\ \frac{1}{M}\\ 0\\ 0\\ 0\end{bmatrix}\begin{bmatrix}\Delta P_m\end{bmatrix}+\begin{bmatrix}0\\ \frac{-K_{pm}}{M}\\ \frac{-K_{qm}}{M}\\ \frac{-K_A K_{vm}}{T_A}\\ K_{DCm}\end{bmatrix}\begin{bmatrix}\Delta m\end{bmatrix} \quad (1)$$

$$z=\begin{bmatrix}1 & 0 & 0 & 0 & 0\\ 0 & 1 & 0 & 0 & 0\\ 0 & 0 & 1 & 0 & 0\\ 0 & 0 & 0 & 1 & 0\\ 0 & 0 & 0 & 0 & 1\end{bmatrix}\begin{bmatrix}\Delta\delta\\ \Delta\omega\\ \Delta E_q^{'}\\ \Delta E_{fd}\\ \Delta V_{DC}\end{bmatrix},$$

$$[y]=[0 \quad 1 \quad 0 \quad 0 \quad 0]\begin{bmatrix}\Delta\delta\\ \Delta\omega\\ \Delta E_q^{'}\\ \Delta E_{fd}\\ \Delta V_{DC}\end{bmatrix} \quad (1)$$

3- Proposed Method:

3- 1- Proposed Controller Structure

Since of the controller structure, there is uncertainty about the parameters and disturbances in the linear system under consideration. Additionally, it is not feasible to measure every state, and even if it were, it would cost more since more sensors would be required. The control system's design ensures that, in the presence of power system disturbances, the linear system with stable output feedback and no external disturbances is asymptotically stable under parameter uncertainty and satisfies the $\frac{z_{L_2}}{w_{L_2}} \le \gamma$ requirement.

Table 2. The parameters related to the single-machine power system and the SSSC [20-25].

Parameter	Definition	Parameter	Definition
X_T	Transformer reactance	V_{DC}	DC voltage of the primary side of the converter
X_L	Reactance of transmission lines	m	Modulation amplitude related to series injected voltage
V_t	Generator bus voltage	ψ	Phase angle corresponding to the series injected voltage
V_b	Infinite bus voltage	V_{INV}	Voltage injected in series into the transmission line
X_{SCT}	Transformer leakage reactance	C_{DC}	DC capacitor capacity

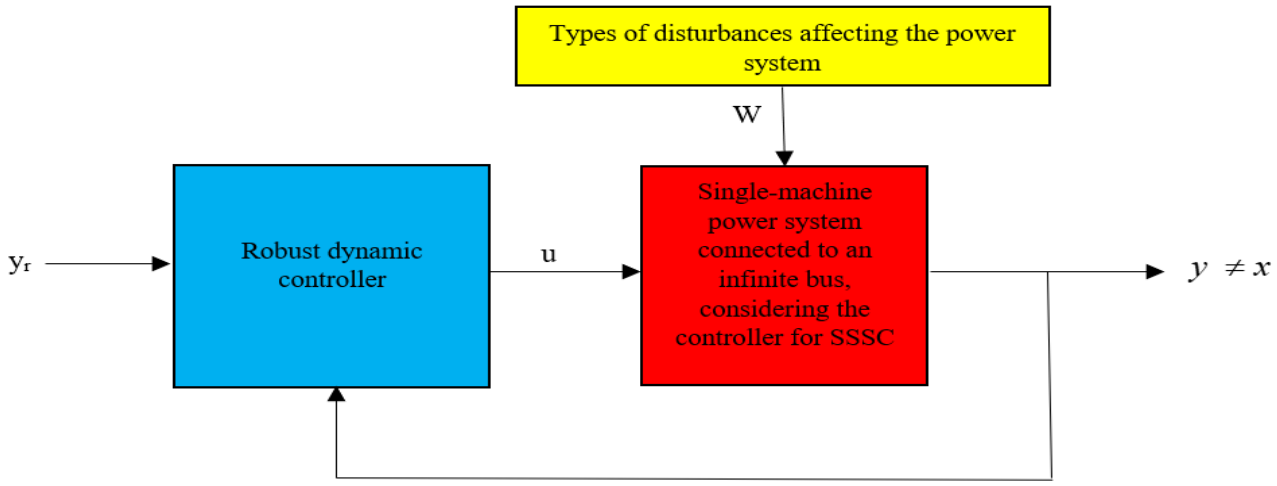

Fig. 3. The topology of power system with a dynamic controller under disturbance and with parameter uncertainty.

The topology of power system with a dynamic controller under disturbance and with parameter uncertainty is depicted in Figure (3). Figure (3) shows that u is the control signal, w is the disturbance entering the system, and y is the system output. Equation (2) is used to represent the linear system's behavior.

$$\begin{aligned} \dot{x} &= A_{n\times n}(t)x_{n\times 1} + B_{n\times m}(t)u_{m\times 1} + D_{n\times d}(t)w_{d\times 1} \\ z &= C_{1_{q\times n}}(t)x_{n\times 1} + D_{11}(t)w + D_{12_{q\times m}}(t)u_{m\times 1} \\ y &= C_2(t)x_{n\times 1} + D_{21}(t)w + D_{22}(t)u, C_2 \neq I \end{aligned} \quad (2)$$

There are n state variables, m control inputs, d disturbances, z adjusted output, y linear system measurement output, and q adjusted outputs in equation (2) [27]. Robust output feedback control is employed in the linear system under investigation since it is not feasible to measure every state simultaneously. In the suggested approach, all of the linear system's parameters may be regarded as unknown and are represented as equation (3) [27–29]. The variable z can be chosen based on the control design requirement.

The uncertainty considered in equation (3) is considered as equation (4), where F(t) is considered as 1×1. The proposed dynamic controller structure for controlling a linear system with uncertainty and disturbance is shown as equation (5).

$$\left\{\begin{array}{l} A(t)=A+\Delta A(t)=A+\Delta A \\ B(t)=B+\Delta B(t)=B+\Delta B \\ D(t)=D+\Delta D(t)=D+\Delta D \\ C_1(t)=C_1+\Delta C_1(t)=C_1+\Delta C_1 \\ D_{12}(t)=D_{12}+\Delta D_{12}(t)=D_{12}+\Delta D_{12} \\ C_2(t)=C_2+\Delta C_2(t)=C_2+\Delta C_2 \end{array}\right\} \quad (3)$$

$$\left\{\begin{array}{l} \Delta A_{n\times n}=M_{A_{n\times 1}}F_{1\times 1}(t)N_{A_{1\times n}} \\ \Delta D_{n\times d}=M_{D_{n\times 1}}F_{1\times 1}(t)N_{D_{1\times d}} \\ \Delta B_{n\times m}=M_{B_{n\times 1}}F_{1\times 1}(t)N_{B_{1\times m}} \\ \Delta C_{1_{q\times n}}=M_{C1_{q\times 1}}F_{1\times 1}(t)N_{C1_{1\times n}} \\ \Delta C_{2_{p\times n}}=M_{C2_{p\times 1}}F_{1\times 1}(t)N_{C2_{1\times n}} \\ \Delta D_{12_{q\times m}}=M_{D12_{q\times 1}}F_{1\times 1}(t)N_{D12_{1\times m}} \\ F^T_{1\times 1}(t)\times F_{1\times 1}(t)\le I\,,F^2(t)\le 1 \end{array}\right\} \quad (4)$$

$$\left\{\begin{array}{l} \dot{\hat{x}}_{n\times 1}=\hat{A}_{n\times n}\hat{x}_{n\times 1}+\hat{B}_{n\times p}\,y_{p\times 1} \\ u_{m\times 1}=\hat{C}_{m\times n}\hat{x}_{n\times 1} \end{array}\right\} \quad (5)$$

Equation (6) illustrates the closed-loop system's structure by fusing equations (2) and (5).

$$\left\{\begin{array}{l} \dot{x}=A(t)x+B(t)\hat{C}\hat{x}+D(t)w \\ z=C_1(t)x+D_{12}(t)\hat{C}\hat{x} \\ \dot{\hat{x}}=\hat{A}\hat{x}+\hat{B}C_2x \end{array}\right\} \quad (6)$$

In equation (6), if, go to zero, the entire closed-loop system is stable. Considering $\bar{x}=\begin{bmatrix} x \\ \hat{x} \end{bmatrix}_{2n\times 1}$, equation (6) is expressed as equation (7).

$$\dot{\bar{x}}=\begin{bmatrix} A(t) & B(t)\hat{C} \\ \hat{B}(t)C_2(t) & \hat{A} \end{bmatrix}_{2n\times 2n}\bar{x} + \begin{bmatrix} D(t) \\ 0 \end{bmatrix}_{2n\times d} w_{d\times 1}=\bar{A}\bar{x}+\bar{D}w \quad (7)$$

3- 2- Control System Objectives:

With the suggested controller, the closed-loop system (linear system with parametric uncertainty and disturbance) aims to achieve two goals:

The closed-loop structure is asymptotically stable under parametric uncertainty in the absence of disruption.

In the presence of disturbance and uncertainty, the closed-loop system achieves the function $\frac{z_{L_2}}{w_{L_2}}\le\gamma$ with zero initial conditions.

To prove the stability of the proposed method, the Lyapunov stability criterion has been used. The Lyapunov stability criterion has been applied for the second objective (with disturbance) and is easily proven for the first objective as well. The Lyapunov criterion and the structure of the closed-loop system are defined as equation (8). Two conditions 8(a) and 8(c) are required for stability based on Lyapunov.

$$\left\{\begin{array}{ll} v=\bar{x}^T p\bar{x}>0\Rightarrow p>0 & (a) \\ \dot{\bar{x}}=\bar{A}\bar{x}+\bar{D}w & (b) \\ \dot{v}=\dot{\bar{x}}^T p\bar{x}+\bar{x}^T p\dot{\bar{x}}=\bar{x}^T\bar{A}^T p\bar{x} & \\ +w^T\bar{D}^T p\bar{x}+\bar{x}^T p\bar{A}\bar{x}+\bar{x}^T p\bar{D}w<0 & (c) \end{array}\right\} \quad (8)$$

To prove condition 8(a), i.e. v>0, the matrix p, p^{-1} is defined according to equation (9) [27-29]. On the other hand, pp^{-1} must be an identity matrix according to equation (10). The linearization matrix is considered as equation (11). According to equation (11), $p\beta_1=\beta_2$, from equation (12) the linear matrix inequality for the first Lyapunov criterion 8(a) is obtained, i.e. if the linear matrix inequality (equation (12)) is greater than zero, the first Lyapunov criterion holds.

$$p=\begin{bmatrix} S_{n\times n} & N_{n\times n} \\ N^T_{n\times n} & U_{n\times n} \end{bmatrix}, p^{-1}=\begin{bmatrix} R_{n\times n} & M_{n\times n} \\ M^T_{n\times n} & T_{n\times n} \end{bmatrix} \quad (9)$$

$$pp^{-1}=\begin{bmatrix} SR+NM^T & SM+NT \\ N^TR+UM^T & N^TM+UT \end{bmatrix}=\begin{bmatrix} I_{n\times n} & 0 \\ 0 & I_{n\times n} \end{bmatrix} \quad (10)$$

$$\beta_1=\begin{bmatrix} R & I \\ M^T & 0 \end{bmatrix}, \beta_2=\begin{bmatrix} I & S \\ 0 & N^T \end{bmatrix} \quad (11)$$

$$\beta_1^T p\beta_1=\beta_1^T\beta_2=\begin{bmatrix} R & M \\ I & 0 \end{bmatrix}\begin{bmatrix} I & S \\ 0 & N^T \end{bmatrix}= \begin{bmatrix} R & RS+MN^T \\ I & S \end{bmatrix}=\begin{bmatrix} R & I \\ I & S \end{bmatrix}>0 \quad (12)$$

Equations (13) through (27) are used to determine the second Lyapunov criteria (8(c)) and transform it into an LMI. The equation $\frac{z_{L_2}}{w_{L_2}}\le\gamma$, which is the criterion for reducing

disturbances to the states of the system under uncertainty, is written according to equation (13).

The second Lyapunov condition, $\dot{v} < 0$, is satisfied by the negativity of the objective function, j. Equation (14) is used to determine the upper band for the goal function j. The function j is negative and the second Lyapunov criteria is also true if equation (15) is true. Consequently, it is necessary to translate equation (15) into the LMI. Equation (15) is converted into equation (16) using substitution and complementation. Since p is symmetric, then $p^T = p$ and $p = \beta_2\beta_1^{-1}$ and according to that equation (16) is transformed into equation (17). Equations (18) and (19) are defined for linearization of equation (17). Linearization of equation (17) is shown according to equation (20). By substituting equation (7) and equation (11) into equation (20), equation (21) is obtained.

$$\begin{cases} \int_0^\infty z^T z \ dt \le \gamma^2 \int_0^\infty w^T w \ dt \\ j = \int_0^\infty (z^T z - \gamma^2 w^T w) dt \le 0 \end{cases} \tag{13}$$

$$\begin{cases} j \le \int_0^\infty (z^T z - \gamma^2 w^T w) dt + v(x(\infty)) - v(x(0)) \\ j \le \int_0^\infty (z^T z - \gamma^2 w^T w + \dot{v}) dt < 0 \end{cases} \tag{14}$$

$$z^T z - \gamma^2 w^T w + \dot{v} < 0 \tag{15}$$

$$\delta_1 = \begin{bmatrix} \bar{A}^T p + p\bar{A} & p\bar{D} & \begin{bmatrix} C_1^T(t) \\ \hat{C}^T D_{12}^T(t) \end{bmatrix} \\ \bar{D}p & \gamma^2 I & 0 \\ \begin{bmatrix} C_1(t) & D_{12}(t)\hat{C} \end{bmatrix} & 0 & -I \end{bmatrix} < 0 \tag{16}$$

$$\delta_2 = \begin{bmatrix} \bar{A}^T \beta_2\beta_1^{-1} + p\bar{A} & \bar{\beta}_1^T \beta_2^T \bar{D} & \begin{bmatrix} C_1^T(t) \\ \hat{C}^T D_{12}^T(t) \end{bmatrix} \\ D\beta_2\beta_1^{-1} & \gamma^2 I & 0 \\ \begin{bmatrix} C_1(t) & D_{12}(t)\hat{C} \end{bmatrix} & 0 & -I \end{bmatrix} < 0 \tag{17}$$

Equation (22) may be inserted into equation (21) to change it into equation (23). Equation (22) uses [27–30] to define parameters $\hat{A}, \hat{B}, \text{and} \hat{C}$, while equation (23) uses distinct matrices to distinguish the fixed values from the unknown parameters. Equation (24) is used to calculate the upper band $o_1 to o_{13}$. The upper band $o_1 to o_{13}$ is obtained from equations (25) and (26), according to equation (26) if $\delta_4 < 0$, $\delta_3 < 0$ and the second Lyapunov criterion is valid. In equation (26) first for $\overline{o_1}$ the Schur complement of the salt is used and it is shown using the Schur complement of equation (27). For o_2 to o_{13} the Schur complement is used like equation (27) and finally it is shown as equation (28).

$$\begin{cases} \delta_2 < 0 \quad , \varsigma^T \delta_2 \varsigma < 0 \\ \varsigma > 0 \end{cases} \tag{18}$$

$$\varsigma = \begin{bmatrix} \beta_1 & 0 & 0 \\ 0 & I & 0 \\ 0 & 0 & I \end{bmatrix}, \varsigma^T = \begin{bmatrix} \beta_1^T & 0 & 0 \\ 0 & I & 0 \\ 0 & 0 & I \end{bmatrix} \tag{19}$$

$$\delta_3 = \begin{bmatrix} \beta_1^T & 0 & 0 \\ 0 & I & 0 \\ 0 & 0 & I \end{bmatrix} \delta_2 \begin{bmatrix} \beta_1 & 0 & 0 \\ 0 & I & 0 \\ 0 & 0 & I \end{bmatrix} = \begin{bmatrix} \beta_1^T \bar{A}^T \beta_2 + \beta_2^T \bar{A} \beta_1 & \beta_2^T \bar{D} & \beta_1^T \begin{bmatrix} C_1^T(t) \\ \hat{C}^T D_{12}^T(t) \end{bmatrix} \\ \bar{D}\beta_2 & \gamma^2 I & 0 \\ \begin{bmatrix} C_1(t) & D_{12}(t)\hat{C} \end{bmatrix} \beta_1 & 0 & -I \end{bmatrix} < 0 \tag{20}$$

$$\delta_3 = \begin{bmatrix} A(t)R + RA^T(t) & A(t) + RA^T(t)S + M\hat{C}^T(t)B^T(t)S & D(t) & RC_1^T(t) \\ +M\hat{C}(t)B^T(t) & +RC_2^T(t)\hat{B}^T(t)N^T + M\hat{A}^T(t)N^T & +M\hat{C}^T(t)D_{12}^T(t) & \\ A^T(t) + SA(t)R & A^T(t)S + SA(t) & SD(t) & C_1^T(t) \\ +SB(t)\hat{C}M^T & +N\hat{B}C_2(t)\hat{B}^T N^T & & \\ +N\hat{B}(t)C_2(t) + N\hat{A}M^T & & & \\ D^T(t) & D^T(t)S & -\gamma^2 I & 0 \\ C_1(t)R + D_{12}(t)\hat{C}M^T & C_1(t) & 0 & -I \end{bmatrix} < 0 \tag{21}$$

$$\begin{cases} \hat{A} = N^{-1}(E - LC_2R \\ -SAR - SBK)M^{-T}, \hat{B} = N^{-1}L \\ \hat{C} = KM^{-T}, A(t) = A + \Delta A, \\ B(t) = B + \Delta B, C(t) = C + \Delta C \end{cases} \tag{22}$$

$$\delta_3 = \begin{bmatrix} AR + RA^T + BK + K^T B^T & A + E^T & D & RC_1^T + K^T D_{12}^T \\ A^T + E & A^T S + SA + LC_2 + C_2^T L^T & SD & C_1^T \\ D^T & D^T S & -\gamma^2 I & 0 \\ C_1 R + D_{12}K & C_1 & 0 & -I \end{bmatrix} + o_1 \tag{23}$$
$$+ o_2 + o_3 + o_4 + o_5 + o_6 + o_7 + o_8 + o_9 + o_{10} + o_{11} + o_{12} + o_{13} < 0$$

$$o_1=\begin{bmatrix}\Delta AR+R\Delta A^T & 0 & 0 & 0\\ 0 & 0 & 0 & 0\\ 0 & 0 & 0 & 0\\ 0 & 0 & 0 & 0\end{bmatrix},o_2=\begin{bmatrix}\Delta BK+K^T\Delta B^T & 0 & 0 & 0\\ 0 & 0 & 0 & 0\\ 0 & 0 & 0 & 0\\ 0 & 0 & 0 & 0\end{bmatrix},$$
$$o_3=\begin{bmatrix}0 & \Delta A & 0 & 0\\ \Delta A^T & 0 & 0 & 0\\ 0 & 0 & 0 & 0\\ 0 & 0 & 0 & 0\end{bmatrix},o_4=\begin{bmatrix}0 & R\Delta A^TS & 0 & 0\\ S\Delta A^TR & 0 & 0 & 0\\ 0 & 0 & 0 & 0\\ 0 & 0 & 0 & 0\end{bmatrix}$$
$$,o_5=\begin{bmatrix}0 & K^T\Delta B^TS & 0 & 0\\ S\Delta BK & 0 & 0 & 0\\ 0 & 0 & 0 & 0\\ 0 & 0 & 0 & 0\end{bmatrix},o_6=\begin{bmatrix}0 & R\Delta C_2^TL^T & 0 & 0\\ L\Delta C_2R & 0 & 0 & 0\\ 0 & 0 & 0 & 0\\ 0 & 0 & 0 & 0\end{bmatrix},$$
$$o_7=\begin{bmatrix}0 & 0 & \Delta D & 0\\ 0 & 0 & 0 & 0\\ \Delta D^T & 0 & 0 & 0\\ 0 & 0 & 0 & 0\end{bmatrix},o_8=\begin{bmatrix}0 & 0 & 0 & R\Delta C_1^T\\ 0 & 0 & 0 & 0\\ 0 & 0 & 0 & 0\\ \Delta C_1R & 0 & 0 & 0\end{bmatrix}$$
$$,o_9=\begin{bmatrix}0 & 0 & 0 & K^T\Delta D_{12}^T\\ 0 & 0 & 0 & 0\\ 0 & 0 & 0 & 0\\ \Delta D_{12}K & 0 & 0 & 0\end{bmatrix},o_{10}=\begin{bmatrix}0 & 0 & 0 & 0\\ 0 & \Delta A^TS+S\Delta A & 0 & 0\\ 0 & 0 & 0 & 0\\ 0 & 0 & 0 & 0\end{bmatrix},\quad (23)$$
$$o_{11}=\begin{bmatrix}0 & 0 & 0 & 0\\ 0 & L\Delta C_2+\Delta C_2^TL^T & 0 & 0\\ 0 & 0 & 0 & 0\\ 0 & 0 & 0 & 0\end{bmatrix},o_{12}=\begin{bmatrix}0 & 0 & 0 & 0\\ 0 & 0 & S\Delta D & 0\\ 0 & \Delta D^TS & 0 & 0\\ 0 & 0 & 0 & 0\end{bmatrix}$$
$$,o_{13}=\begin{bmatrix}0 & 0 & 0 & 0\\ 0 & 0 & 0 & \Delta C_1^T\\ 0 & 0 & 0 & 0\\ 0 & 0 & \Delta C_1 & 0\end{bmatrix},$$
$$o=\begin{bmatrix}AR+RA^T+BK+K^TB^T & A+E^T & D & RC_1^T+K^TD_{12}^T\\ A^T+E & A^TS+SA+LC_2+C_2^TL^T & SD & C_1^T\\ D^T & D^TS & -\gamma^2I & 0\\ C_1R+D_{12}K & C_1 & 0 & -I\end{bmatrix}$$

$$\sigma F\upsilon+\upsilon^TF^T\sigma^T\le\Gamma\sigma\sigma^T+\Gamma^{-1}\upsilon^T\upsilon,F^TF\le I \quad (24)$$

$$\begin{aligned}
&o_1=\sigma_1F\upsilon_1+\upsilon_1^TF^T\sigma_1^T\le\Gamma_1\sigma_1\sigma_1^T+\Gamma_1^{-1}\upsilon_1^T\upsilon_1,o_2=\\
&\quad\sigma_2F\upsilon_2+\upsilon_2^TF^T\sigma_2^T\le\Gamma_2\sigma_2\sigma_2^T+\Gamma_2^{-1}\upsilon_2^T\upsilon_3\\
&o_3=\sigma_3F\upsilon_3+\upsilon_3^TF^T\sigma_3^T\le\Gamma_3\sigma_3\sigma_1^T+\Gamma_3^{-1}\upsilon_3^T\upsilon_3,o_4=\\
&\quad\sigma_4F\upsilon_4+\upsilon_4^TF^T\sigma_4^T\le\Phi_1\sigma_4\sigma_4^T+\Phi_1^{-1}\upsilon_4^T\upsilon_4\\
&o_5=\sigma_5F\upsilon_5+\upsilon_5^TF^T\sigma_5^T\le\Phi_2\sigma_5\sigma_5^T+\Phi_2^{-1}\upsilon_5^T\upsilon_5,o_6=\\
&\quad\sigma_6F\upsilon_6+\upsilon_6^TF^T\sigma_6^T\le\Phi_3\sigma_6\sigma_6^T+\Phi_3^{-1}\upsilon_6^T\upsilon_6\\
&o_7=\sigma_7F\upsilon_7+\upsilon_7^TF^T\sigma_7^T\le\Gamma_4\sigma_7\sigma_7^T+\Gamma_4^{-1}\upsilon_7^T\upsilon_7,o_8=\\
&\quad\sigma_8F\upsilon_8+\upsilon_8^TF^T\sigma_8^T\le\Gamma_5\sigma_8\sigma_8^T+\Gamma_5^{-1}\upsilon_8^T\upsilon_8\\
&o_9=\sigma_9F\upsilon_9+\upsilon_9^TF^T\sigma_9^T\le\Gamma_6\sigma_9\sigma_9^T+\Gamma_6^{-1}\upsilon_9^T\upsilon_9,o_{10}=\\
&\quad\sigma_{10}F\upsilon_{10}+\upsilon_{10}^TF^T\sigma_{10}^T\le\Gamma_7\sigma_{10}\sigma_{10}^T+\Gamma_7^{-1}\upsilon_{10}^T\upsilon_{10}\\
&o_{11}=\sigma_{11}F\upsilon_{11}+\upsilon_{11}^TF^T\sigma_{11}^T\le\Gamma_8\sigma_{11}\sigma_{11}^T+\Gamma_8^{-1}\upsilon_{11}^T\upsilon_{11},o_{12}=\\
&\quad\sigma_{12}F\upsilon_{12}+\upsilon_{12}^TF^T\sigma_{12}^T\le\Gamma_9\sigma_{12}\sigma_{12}^T+\Gamma_9^{-1}\upsilon_{12}^T\upsilon_{12}\\
&o_{13}=\sigma_{13}F\upsilon_{13}+\upsilon_{13}^TF^T\sigma_{13}^T\le\Gamma_{10}\sigma_{13}\sigma_{13}^T+\Gamma_{10}^{-1}\upsilon_{13}^T\upsilon_{13}
\end{aligned} \quad (25)$$

$$\sigma_1=\begin{bmatrix}M_A\\0\\0\\0\end{bmatrix},\upsilon_1=\begin{bmatrix}N_AR & 0 & 0 & 0\end{bmatrix},$$
$$\sigma_2=\begin{bmatrix}M_B\\0\\0\\0\end{bmatrix},\upsilon_2=\begin{bmatrix}0 & N_A & 0 & 0\end{bmatrix}$$
$$\sigma_3=\begin{bmatrix}M_A\\0\\0\\0\end{bmatrix},\upsilon_3=\begin{bmatrix}0 & N_A & 0 & 0\end{bmatrix},$$
$$\sigma_4=\begin{bmatrix}0\\SM_A\\0\\0\end{bmatrix},\upsilon_4=\begin{bmatrix}N_AR & 0 & 0 & 0\end{bmatrix}$$
$$\sigma_5=\begin{bmatrix}0\\SM_B\\0\\0\end{bmatrix},\upsilon_5=\begin{bmatrix}N_BK & 0 & 0 & 0\end{bmatrix},$$
$$\sigma_6=\begin{bmatrix}0\\LM_{C_2}\\0\\0\end{bmatrix},\upsilon_6=\begin{bmatrix}N_{C_2}R & 0 & 0 & 0\end{bmatrix}$$
$$\sigma_7=\begin{bmatrix}M_D\\0\\0\\0\end{bmatrix},\upsilon_7=\begin{bmatrix}0 & 0 & N_D & 0\end{bmatrix},$$
$$\sigma_8=\begin{bmatrix}0\\0\\0\\M_{C_1}\end{bmatrix},\upsilon_8=\begin{bmatrix}N_{C_1}R & 0 & 0 & 0\end{bmatrix}$$
$$\sigma_9=\begin{bmatrix}0\\0\\0\\M_{D_{12}}\end{bmatrix},\upsilon_9=\begin{bmatrix}N_{D_{12}}K & 0 & 0 & 0\end{bmatrix},$$
$$\sigma_{10}=\begin{bmatrix}0\\SM_A\\0\\0\end{bmatrix},\upsilon_{10}=\begin{bmatrix}0 & N_A & 0 & 0\end{bmatrix}$$
$$\sigma_{11}=\begin{bmatrix}0\\LM_{C_2}\\0\\0\end{bmatrix},\upsilon_{11}=\begin{bmatrix}0 & N_{C_2} & 0 & 0\end{bmatrix},$$
$$\sigma_{12}=\begin{bmatrix}0\\SM_D\\0\\0\end{bmatrix},\upsilon_{12}=\begin{bmatrix}0 & 0 & N_D & 0\end{bmatrix}$$

$$(\sigma_{13}=\begin{bmatrix}0\\0\\0\\M_{C_1}\end{bmatrix},\upsilon_{13}=\begin{bmatrix}0 & N_{C_1} & 0 & 0\end{bmatrix},$$

$$\bar{o}_1=\Gamma_1\sigma_1\sigma_1^T+\Gamma_1^{-1}\upsilon_1^T\upsilon_1,\bar{o}_2=\Gamma_2\sigma_2\sigma_2^T+\Gamma_2^{-1}\upsilon_2^T\upsilon_2$$

$$\begin{aligned}
\bar{o}_3&=\Gamma_3\sigma_3\sigma_3^T+\Gamma_3^{-1}\upsilon_3^T\upsilon_3,\\
\bar{o}_4&=\Phi_1\sigma_4\sigma_4^T+\Phi_1^{-1}\upsilon_4^T\upsilon_4,\\
\bar{o}_5&=\Phi_2\sigma_5\sigma_5^T+\Phi_2^{-1}\upsilon_5^T\upsilon_5,\\
\bar{o}_6&=\Phi_3\sigma_6\sigma_6^T+\Phi_3^{-1}\upsilon_6^T\upsilon_6,\\
\bar{o}_7&=\Gamma_4\sigma_7\sigma_7^T+\Gamma_4^{-1}\upsilon_7^T\upsilon_7,\\
\bar{o}_8&=\Gamma_5\sigma_8\sigma_8^T+\Gamma_5^{-1}\upsilon_8^T\upsilon_8,\\
\bar{o}_9&=\Gamma_6\sigma_9\sigma_9^T+\Gamma_6^{-1}\upsilon_9^T\upsilon_9,\\
\bar{o}_{10}&=\Gamma_7\sigma_{10}\sigma_{10}^T+\Gamma_7^{-1}\upsilon_{10}^T\upsilon_{10}\\
,\bar{o}_{11}&=\Gamma_8\sigma_{11}\sigma_{11}^T+\Gamma_8^{-1}\upsilon_{11}^T\upsilon_{11},\\
\bar{o}_{12}&=\Gamma_9\sigma_{12}\sigma_{12}^T+\Gamma_9^{-1}\upsilon_{12}^T\upsilon_{12},\\
\bar{o}_{13}&=\Gamma_{10}\sigma_{13}\sigma_{13}^T+\Gamma_{10}^{-1}\upsilon_{13}^T\upsilon_{13}
\end{aligned}\qquad(25)$$

$$\delta_3\le o+\sum_{i=1}^{13}\bar{o}_i=\delta_4<0\qquad(26)$$

$$\delta_4=o+\sum_{i=2}^{13}\bar{o}_i+\begin{bmatrix}\Gamma_1M_AM_A^T & 0 & 0 & 0\\ 0 & 0 & 0 & 0\\ 0 & 0 & 0 & 0\\ 0 & 0 & 0 & 0\end{bmatrix}+\begin{bmatrix}RN_A^T\\0\\0\\0\end{bmatrix}\Gamma_1^{-1}\begin{bmatrix}N_AR & 0 & 0 & 0\end{bmatrix}<0\qquad(27)$$

$$\delta_4=\begin{bmatrix}o+\sum_{i=2}^{13}\bar{o}_i & \begin{bmatrix}RN_A^T\\0\\0\\0\end{bmatrix}\\ \begin{bmatrix}N_AR & 0 & 0 & 0\end{bmatrix} & -\Gamma_1\end{bmatrix}<0$$

$$\delta_4=\begin{bmatrix}
\delta_{11_{n\times n}} & A+E^T & D & RC_1^T+KD_{12}^T & RN_A^T & K^TN_B^T & 0_{n\times1} & 0_{n\times1} & RN_{C_1}^T & KN_{D_{12}}^T & 0_{n\times1} & 0_{n\times1} & 0_{n\times1} & 0_{n\times1} & 0_{n\times1} & RN_A^T & 0_{n\times1} & K^TN_B^T & 0_{n\times1} & RN_{C_2}^T\\
A^T+E & \delta_{22_{n\times n}} & SD & C_1^T & 0_{n\times1} & 0_{n\times1} & N_A^T & 0_{n\times1} & 0_{n\times1} & 0_{n\times1} & SM_A & LM_{C_2} & SN_D & N_{C_1}^T & SM_A & 0_{n\times1} & SM_B & 0_{n\times1} & LM_{C_2} & 0_{n\times1}\\
D & D^TS & \delta_{33_{d\times d}} & 0_{d\times q} & 0_{d\times1} & 0_{d\times1} & N_D^T & 0_{d\times1} & 0_{d\times1} & 0_{d\times1} & 0_{d\times1} & 0_{d\times1} & 0_{d\times1} & 0_{d\times1} & 0_{d\times1} & 0_{d\times1} & 0_{d\times1} & 0_{d\times1} & 0_{d\times1} & 0_{d\times1}\\
C_1R+D_{12}K & C_1 & 0_{q\times d} & \delta_{44_{q\times q}} & 0_{q\times1} & 0_{q\times1} & 0_{q\times1} & 0_{q\times1} & 0_{q\times1} & 0_{q\times1} & 0_{q\times1} & 0_{q\times1} & 0_{q\times1} & 0_{q\times1} & 0_{q\times1} & 0_{q\times1} & 0_{q\times1} & 0_{q\times1} & 0_{q\times1} & 0_{q\times1}\\
N_AR & 0_{1\times n} & 0_{1\times d} & 0_{1\times q} & -\Gamma_1 & 0 & 0 & 0 & 0 & 0 & 0 & 0 & 0 & 0 & 0 & 0 & 0 & 0 & 0 & 0\\
N_BK & 0_{1\times n} & 0_{1\times d} & 0_{1\times q} & 0 & -\Gamma_2 & 0 & 0 & 0 & 0 & 0 & 0 & 0 & 0 & 0 & 0 & 0 & 0 & 0 & 0\\
0_{1\times n} & N_A & 0_{1\times d} & 0_{1\times q} & 0 & 0 & -\Gamma_3 & 0 & 0 & 0 & 0 & 0 & 0 & 0 & 0 & 0 & 0 & 0 & 0 & 0\\
0_{1\times n} & 0_{1\times n} & N_D & 0_{1\times q} & 0 & 0 & 0 & -\Gamma_4 & 0 & 0 & 0 & 0 & 0 & 0 & 0 & 0 & 0 & 0 & 0 & 0\\
N_{C_1}R & 0_{1\times n} & 0_{1\times d} & 0_{1\times q} & 0 & 0 & 0 & 0 & -\Gamma_5 & 0 & 0 & 0 & 0 & 0 & 0 & 0 & 0 & 0 & 0 & 0\\
N_{D_{12}}K & 0_{1\times n} & 0_{1\times d} & 0_{1\times q} & 0 & 0 & 0 & 0 & 0 & -\Gamma_6 & 0 & 0 & 0 & 0 & 0 & 0 & 0 & 0 & 0 & 0\\
0_{1\times n} & M_A^TS & 0_{1\times d} & 0_{1\times q} & 0 & 0 & 0 & 0 & 0 & 0 & -\Gamma_7 & 0 & 0 & 0 & 0 & 0 & 0 & 0 & 0 & 0\\
0_{1\times n} & M_{C_2}^TL^T & 0_{1\times d} & 0_{1\times q} & 0 & 0 & 0 & 0 & 0 & 0 & 0 & -\Gamma_8 & 0 & 0 & 0 & 0 & 0 & 0 & 0 & 0\\
0_{1\times n} & M_D^TS & 0_{1\times d} & 0_{1\times q} & 0 & 0 & 0 & 0 & 0 & 0 & 0 & 0 & -\Gamma_9 & 0 & 0 & 0 & 0 & 0 & 0 & 0\\
0_{1\times n} & N_{C_1} & 0_{1\times d} & 0_{1\times q} & 0 & 0 & 0 & 0 & 0 & 0 & 0 & 0 & 0 & -\Gamma_{10} & 0 & 0 & 0 & 0 & 0 & 0\\
0_{1\times n} & M_A^TS & 0_{1\times d} & 0_{1\times q} & 0 & 0 & 0 & 0 & 0 & 0 & 0 & 0 & 0 & 0 & -\Phi_1^{-1} & 0 & 0 & 0 & 0 & 0\\
N_AR & 0_{1\times n} & 0_{1\times d} & 0_{1\times q} & 0 & 0 & 0 & 0 & 0 & 0 & 0 & 0 & 0 & 0 & 0 & -\Phi_1 & 0 & 0 & 0 & 0\\
0_{1\times n} & M_B^TS & 0_{1\times d} & 0_{1\times q} & 0 & 0 & 0 & 0 & 0 & 0 & 0 & 0 & 0 & 0 & 0 & 0 & -\Phi_2^{-1} & 0 & 0 & 0\\
N_BK & 0_{1\times n} & 0_{1\times d} & 0_{1\times q} & 0 & 0 & 0 & 0 & 0 & 0 & 0 & 0 & 0 & 0 & 0 & 0 & 0 & -\Phi_2 & 0 & 0\\
0_{1\times n} & M_{C_2}^TL^T & 0_{1\times d} & 0_{1\times q} & 0 & 0 & 0 & 0 & 0 & 0 & 0 & 0 & 0 & 0 & 0 & 0 & 0 & 0 & -\Phi_3^{-1} & 0\\
N_{C_2}R & 0_{1\times n} & 0_{1\times d} & 0_{1\times q} & 0 & 0 & 0 & 0 & 0 & 0 & 0 & 0 & 0 & 0 & 0 & 0 & 0 & 0 & 0 & -\Phi_3
\end{bmatrix}<0\qquad(28)$$

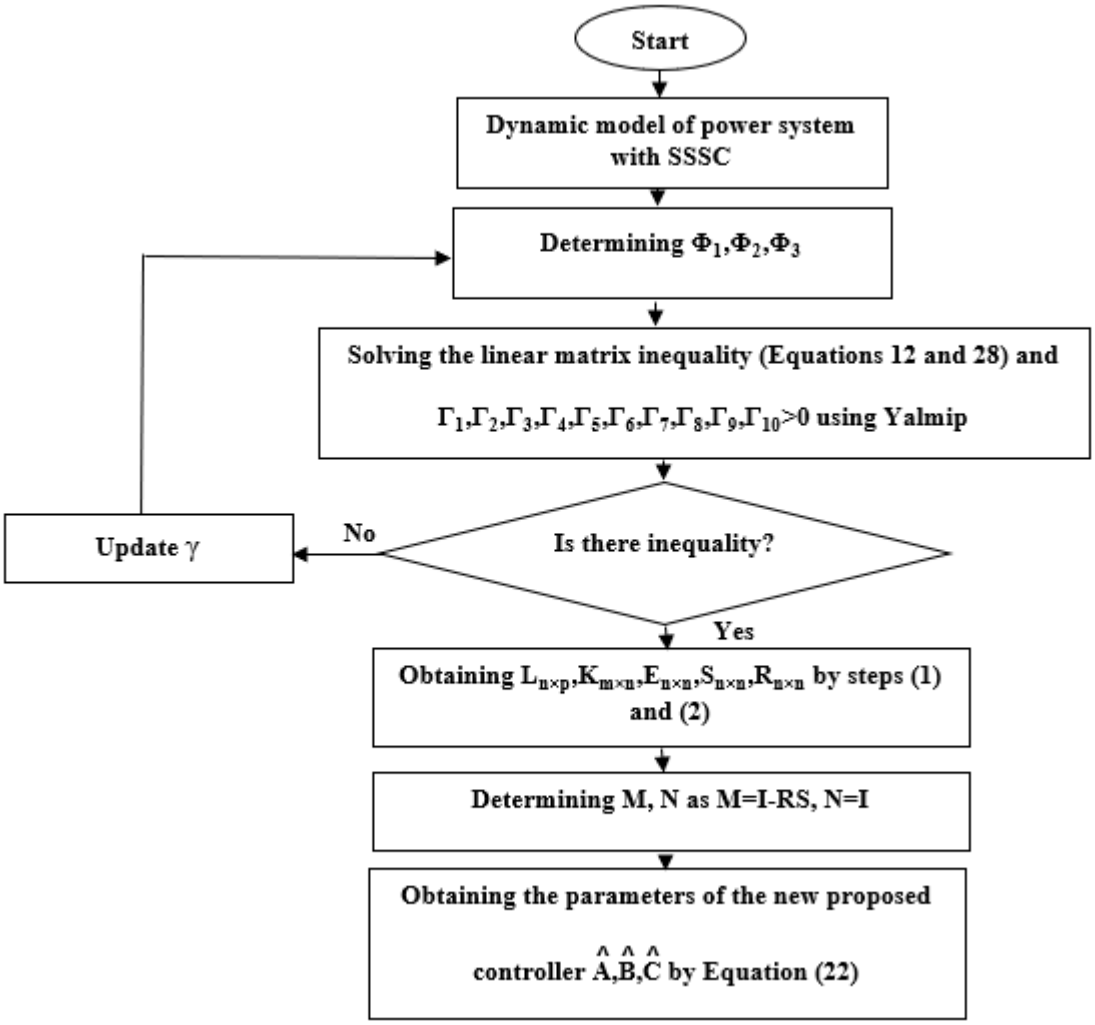

Fig. 4. The flowchart of the proposed method.

3- 3- Steps to Design the New Proposed Controller:

1) Determining $\ddot{O}_1,\ddot{O}_2,\ddot{O}_3$
2) Solving the linear matrix inequality (Equations 12 and 28) and $\tilde{A}_1,\tilde{A}_2,\tilde{A}_3,\tilde{A}_4,\tilde{A}_5,\tilde{A}_6,\tilde{A}_7,\tilde{A}_8,\tilde{A}_9,\tilde{A}_{10}>0$ using Yalmip
3) Obtaining $L_{n\times p},K_{m\times n},E_{n\times n},S_{n\times n},R_{n\times n}$ by steps (1) and (2)
4) Determining M, N as M=I-RS, N=I
5) Obtaining the parameters of the new proposed controller $\hat{A},\hat{B},\hat{C}$ by Equation (21)

The flowchart of the proposed method is shown in Figure (4).

3- 4- SSSC Based on the Proposed Method

A modest signal model has been employed to lower the power system's LFOs. Equation (29), which takes into account the controller for SSSC using the Heffron-Phillips model, displays the small signal model of a single-machine power system connected to an infinite bus. In the system under study, $D_{11}=D_{12_{q\times m}}=D_{21}=D_{22}=0$. The goal in designing the proposed controller is to damp the LFOs of the power system by considering the uncertainty in the parameters of the power system (parameter uncertainty) and the disturbances entering the power system. The modulation amplitude of the SSSC, which is indicated by the index m, provides a control signal Δm for better damping of the power system oscillations. The characteristics of the power system are shown in Table (3).

$$A=\begin{bmatrix} 0 & \omega_0 & 0 & 0 & 0 \\ \frac{-K_1}{M} & \frac{-D}{M} & \frac{-K_2}{M} & 0 & \frac{-K_{pDC}}{M} \\ \frac{-K_4}{T_{do}^{'}} & 0 & \frac{-K_3}{T_{do}^{'}} & \frac{1}{T_{do}^{'}} & \frac{-K_{dDC}}{T_{do}^{'}} \\ \frac{-K_A K_5}{T_A} & 0 & \frac{-K_A K_6}{T_A} & \frac{-1}{T_A} & \frac{-K_A K_{vDC}}{T_A} \\ K_7 & 0 & K_8 & 0 & -K_9 \end{bmatrix}, \quad (29)$$

Table 3. The characteristics of the power system.

Variable	value	Variable	value
M	$6\frac{MJ}{MVA}$	P_e	$8\,pu$
D	**0**	Q_e	$0.144\,pu$
T'_{d0}	$5.044s$	V_b	$1\,pu$
X_d	$0.1\,pu$	K_{pm}	0.0839
X_q	$0.06\,pu$	K_1	1.9014
X'_d	$0.025\,pu$	K_2	0.6735
f_0	$60\,Hz$	K_3	1.1429
ω_0	$2\pi f_0$	K_4	0.0498
K_A	5	K_5	–0.0127
T_A	0.005	K_6	0.9517
K_7	–0.1759	K_{pDC}	0.0244
K_8	0.302	K_{qDC}	0.806
K_9	0.00014	K_{vDC}	–0.0035
K_{qm}	0.0354	K_{vm}	–0.008
K_{DCm}	–0.4255		

$$B=\begin{bmatrix}0\\ \frac{-K_{pm}}{M}\\ \frac{-K_{qm}}{M}\\ \frac{-K_A K_{vm}}{T_A}\\ K_{DCm}\end{bmatrix},D=\begin{bmatrix}0\\ \frac{1}{M}\\ 0\\ 0\\ 0\end{bmatrix}$$

$$,C_1=\begin{bmatrix}1&0&0&0&0\\0&1&0&0&0\\0&0&1&0&0\\0&0&0&1&0\\0&0&0&0&1\end{bmatrix},$$

$$C_2=\begin{bmatrix}0&1&0&0&0\end{bmatrix}$$

4- Simulation:

The SSSC equipped with the proposed controller in the power system for damping oscillations is compared with SSSC(RMPC) methods, fuzzy lead-lag control optimized by PSO, and fuzzy lead-lag control optimized by MWOA. In the first scenario, mild disturbances in the power system are investigated by considering the proposed controller and other various controllers. In the second scenario, mild disturbances and mild uncertainty in the power system parameters (inertia (M) of -30%) are investigated and the proposed controller and other controllers are compared. In the third scenario, severe disturbances in the power system are investigated by considering the proposed controller and other various controllers. In the fourth scenario, the proposed controller and other controllers are compared to study severe disturbances and severe uncertainty in power system parameters (inertia (M) of -50%). The desired dynamic controller parameters for the power system are obtained according to the proposed new method according to equations (30), (31) and (32).

$$\hat{A}=\begin{bmatrix}-9.5228&-6.5085&1.1566&-1.5632&-10.6\\-13.428&-14.018&2.341&-34.964&-16.816\\-323.88&-46.549&10.215&-14.06&-74.537\\11.44&22.236&-5.1964&-109.92&35.58\\-63.039&-93.715&20.794&-18.574&-15.009\end{bmatrix} \quad (30)$$

$$\hat{B}=\begin{bmatrix}-11.448\\-88.254\\-38.959\\22.02\\-87.364\end{bmatrix} \quad (31)$$

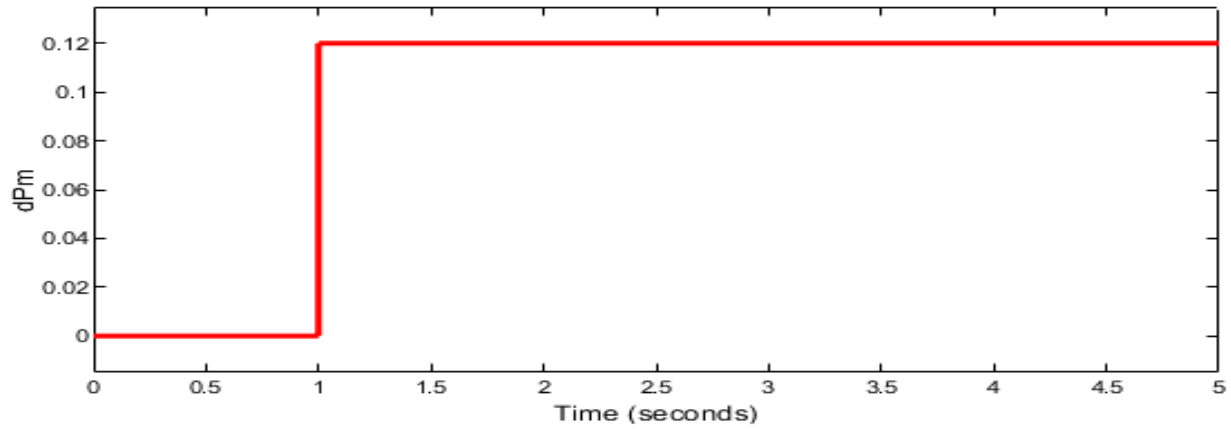

Fig. 5. The mild disturbance is applied to the power system.

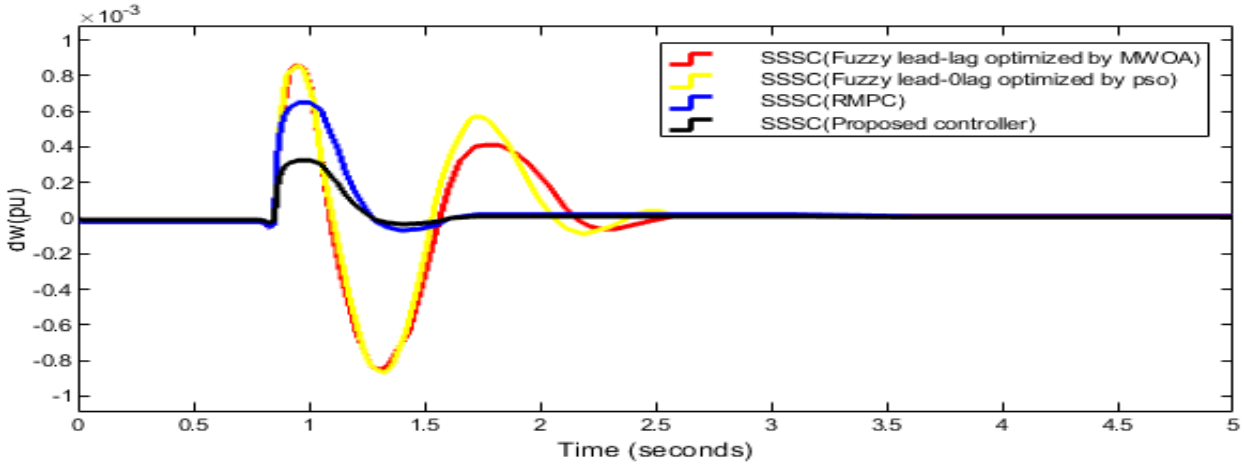

Fig. 6. The changes in the rotor angular velocity over time and based on different controllers , Scenario 1.

$$\hat{C} = [-0.21396 \quad -0.31979 \quad 0.070286 \quad -1.3156 \quad -0.5116] \quad (32)$$

Scenario 1: Given that in this scenario, the effect of mild disturbances in the power system is considered. First, according to Figure (5), a mild disturbance is applied to the power system. In Figure (6), the changes in the rotor angular velocity over time and based on different controllers are shown. According to Figure (6), the SSSC equipped with the proposed controller in the power system for damping oscillations has better performance in terms of response speed, reduction of overshoot and reduction of undershoot compared to SSSC(RMPC), fuzzy lead-lag control optimized by PSO, and fuzzy lead-lag control optimized by MWOA.

Scenario 2: In this scenario, mild disturbances and mild uncertainty in power system parameters (inertia (M) of -30%) are investigated by comparing the proposed controller and other controllers. First, according to Figure (5), mild disturbances are applied to the power system. In Figure (7), the changes in the rotor angular velocity over time and based on different controllers are shown. According to Figure (7), the SSSC equipped with the proposed controller in the power system for damping oscillations has better performance in terms of response speed, reduction of inflection and reduction of overturning compared to SSSC(RMPC), fuzzy lead-lag control optimized by PSO, and fuzzy lead-lag control optimized by MWOA. Also, the proposed method has been able to be robust against mild disturbances and mild uncertainty related to system parameters. The results of scenarios (1) and (2) for different controllers from the ST, MO, and MU are shown in Table (4).

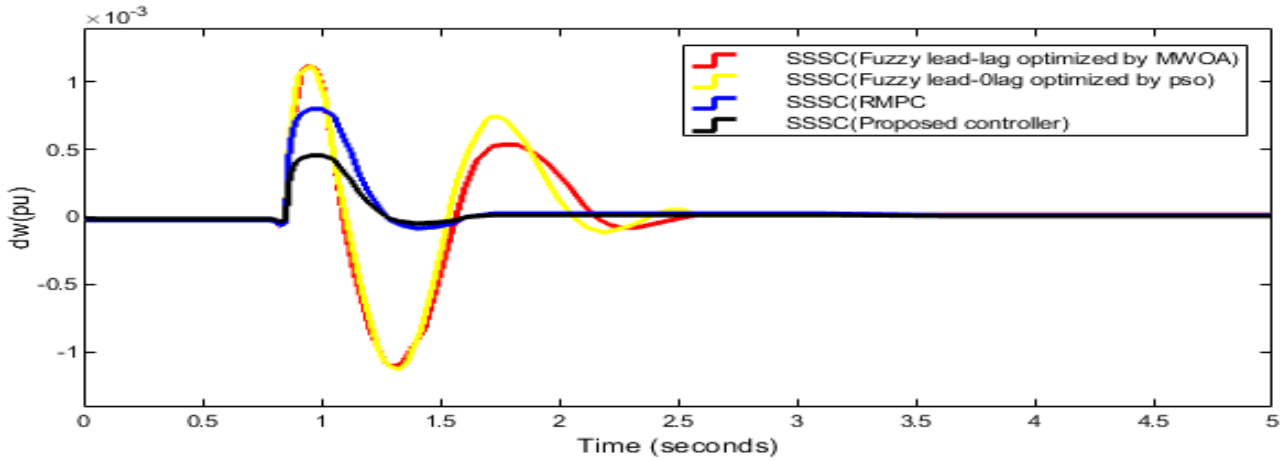

Fig. 7. The changes in the rotor angular velocity over time and based on different controllers , Scenario 2.

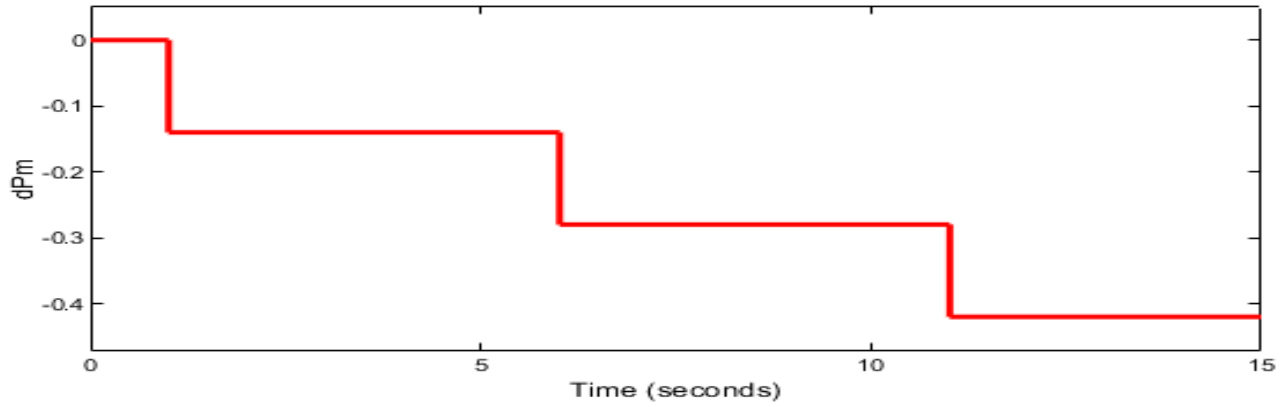

Fig. 8. The severe disturbance is applied to the power system, Scenario 3.

Scenario 3: In this scenario, severe disturbances are investigated by comparing the proposed controller with other controllers. First, as shown in Figure (8), a severe disturbance is applied to the power system. In Figure (9), the changes in the rotor angular velocity over time and based on different controllers are shown. According to Figure (9), the SSSC equipped with the proposed controller in the power system for damping oscillations has better performance in terms of response speed, reduction of inflection and reduction of overturning compared to SSSC(RMPC), fuzzy lead-lag control optimized by PSO, and fuzzy lead-lag control optimized by MWOA. Additionally, the suggested approach has shown resilient to significant disruptions associated with system characteristics.

Scenario 4: In this scenario, the proposed controller and other controllers are compared to study severe disturbances and severe uncertainty in power system parameters (inertia (M) of -50%). First, according to Figure (8), severe disturbance is applied to the power system. In Figure (10), the changes in rotor angular velocity over time and based on different controllers are shown. According to Figure (10), the SSSC equipped with the proposed controller in the power system for damping oscillations has better performance in terms of response speed, reduction of inflection and reduction of overturning compared to static series compensation based on to SSSC(RMPC), fuzzy lead-lag control optimized by PSO, and fuzzy lead-lag control optimized by MWOA. Also, the proposed method has been able to be resistant to severe disturbances and severe uncertainty related to system parameters. The results of scenarios (3) and (4) for different controllers from the ST, MO, and MU are shown in Table (5).

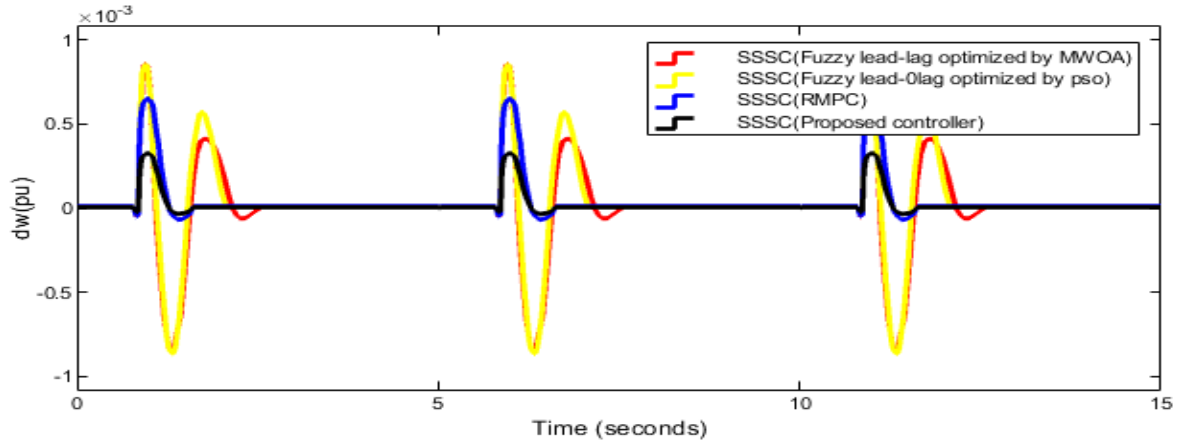

Fig. 9. The changes in the rotor angular velocity over time and based on different controllers, Scenario 3.

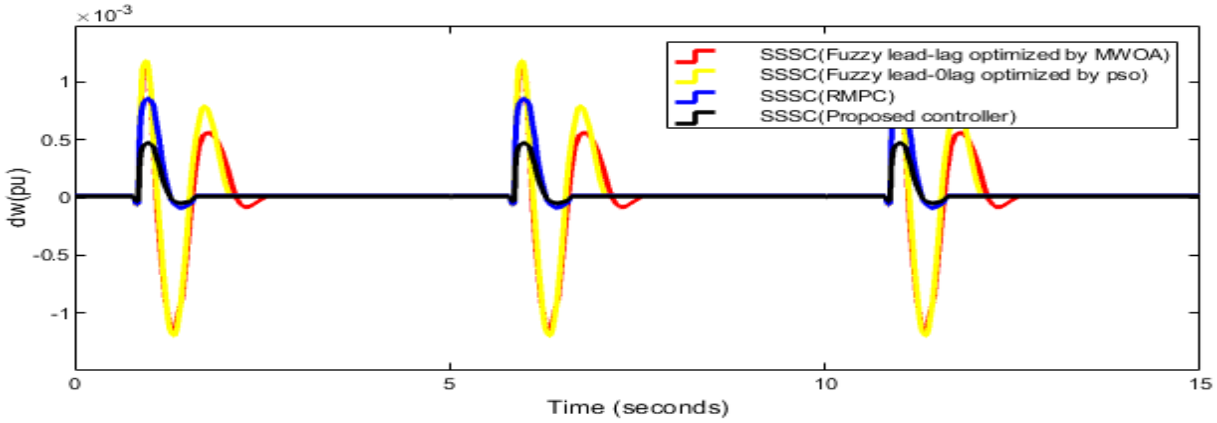

Fig. 10. The changes in the rotor angular velocity over time and based on different controllers, Scenario 3.

Table 4. The results of scenarios (1) and (2) for different controllers.

SSSC based on controller	Scenario 1			Scenario 2		
	MO (pu)	MU (pu)	ST (sec)	MO (pu)	MU (pu)	ST (sec)
SSSC (Proposed controller)	3×10^{-4}	10^{-5}	0.93	3.2×10^{-4}	10^{-5}	0.95
SSSC(RMPC)	7×10^{-4}	2×10^{-5}	0.98	8×10^{-4}	2.1×10^{-5}	1.05
SSSC (Fuzzy lead-lag optimized by PSO)	9×10^{-4}	9×10^{-4}	1.53	12×10^{-4}	12×10^{-4}	1.58
SSSC (Fuzzy lead-lag optimized by MWOA)	9×10^{-4}	9×10^{-4}	1.59	13×10^{-4}	12×10^{-4}	1.62

Table 5. The results of scenarios (3) and (4) for different controllers.

SSSC based on controller	Scenario 3			Scenario 4		
	MO (pu)	MU (pu)	ST (sec)	MO (pu)	MU (pu)	ST (sec)
SSSC(Proposed controller)	3.1×10^{-4}	10^{-5}	0.95	3.4×10^{-4}	10^{-5}	0.97
SSSC(RMPC)	7.3×10^{-4}	2.3×10^{-5}	0.99	8.4×10^{-4}	2.5×10^{-5}	1.07
SSSC(Fuzzy lead-lag optimized by PSO)	9.5×10^{-4}	9.2×10^{-4}	1.56	13.3×10^{-4}	12.2×10^{-4}	1.6
SSSC(Fuzzy lead-lag optimized by MWOA)	9.4×10^{-4}	9.3×10^{-4}	1.61	13.2×10^{-4}	12.2×10^{-4}	1.65

5- Conclusion:

According to this paper, a novel robust controller with an output feedback based on LMI was created for an SSSC in order to decrease LFOs and increase power system stability. The SSSC equipped with the output feedback method based LMI was compared with compensation based on SSSC(RMPC), fuzzy lead-lag control optimized by PSO, and fuzzy lead-lag control optimized by MWOA. The results show that the proposed method has a favorable performance compared to other control methods presented and is able to be resistant to parameter uncertainty and disturbances. The maximum deviations related to the rotor angular velocity are improved by 58% using the proposed method. The settling time related to rotor angular velocity deviations has been improved by 6% using the proposed method.

Abbreviations

SSSC	static synchronous series compensator
LFC	Load frequency control
LMI	linear matrix inequality
MPC	Model predictive control
PSO	Particle swarm optimization
MWOA	Modified whale optimization algorithm
LFOs	low-frequency oscillations
GA	genetic algorithm
COA	colony optimization algorithm
GWO	Grey Wolf Optimization
RMPC	Robust Model predictive control
ST	settling time
MO	Maximum overshoot
MU	Maximum undershoot

Data availability statement: Data are contained within the article.

References

[1] Hong, X., Mitchell, R. J., Chen, S., Harris, C. J., Li, K., & Irwin, G. W. (2008). Model selection approaches for non-linear system identification: a review. International journal of systems science, 39(10), 925-946.

[2] Amiri, F., Moradi, M. H., & Eskandari, M. (2024). Suppression of low-frequency oscillations in hybrid/multi microgrid systems with an improved model predictive controller. IET Renewable Power Generation, 18(9-10), 1691-1709.

[3] Ngei, U. M., Nyete, A. M., Moses, P. M., & Wekesa, C. (2024). Optimal sizing and placement of STATCOM, TCSC and UPFC using a novel hybrid genetic algorithm-improved particle swarm optimization. Heliyon, 10(23).

[4] Barua, P., Shekher, V., Kumar, V., Ansari, M. F., Alguno, A. C., & Barua, R. (2023). Rotor angle stability and voltage stability improvement of highly renewable energy penetrated western grid of Bangladesh power system using FACTS device. Cogent Engineering, 10(1), 2210899.

[5] Roy, C., Chatterjee, D., & Bhattacharya, T. (2023). Control of a hybrid shunt FACTS compensator for voltage collapse prevention in interconnected EHV power transmission systems. IEEE Journal of Emerging and Selected Topics in Industrial Electronics, 4(2), 538-548.

[6] Chen, Y., Wang, D., Li, J., Fan, H., Li, J., Luo, Y., & Li, L. (2023). A SSSC optimal configuration method to

enhance available transfer capability considering multi-wind farm access. IET Renewable Power Generation, 17(16), 3777-3792.

[7] Sadiq, E. H., Mohammed, L. A., & Taha, H. M. (2024). Enhancing power transmission efficiency using static synchronous series compensators: a comprehensive review. Journal of Intelligent Systems and Control, 3(2), 71-83.

[8] Ma, T., Wang, S., Yang, S., & Aliev, H. (2024). Enhanced Voltage Drop Compensation in Wind-Driven Microgrids Using a Hybrid Dual-Vector Controller and SSSC. IEEE Access.

[9] Kalyan, C. N. S., Tellapati, A. D., Kalyani, T. V. S., Rao, K. V. G., Goud, B. S., & Mandadi, P. N. (2024, March). BES and SSSC Based Supplementary Control for Frequency Regulation of Multi Area Interconnected Power System Network. In 2024 International Conference on Distributed Computing and Optimization Techniques (ICDCOT) (pp. 1-6). IEEE.

[10] Rohit, C., Darji, P., & Jariwala, H. R. (2023). A preordainment approach for design of auxiliary damping controller and SSSC tuning to enhance SSR mode stability in DFIG based windfarm. Smart Science, 11(3), 605-628.

[11] Patra, S. K., & Mohapatra, S. K. (2023). Power System Stability by Improved Grasshopper Optimization Algorithm-Based PSS with Type-2 Fuzzy Lead-Lag based SSSC Controller. Journal of Engineering Science & Technology Review, 16(6).

[12] Bhukya, J., & Alam, M. (2024). Dynamic stability reinforcement in remote wind farm connections: POD-SSSC coordination with fuzzy logic control using RTDS. Electrical Engineering, 106(3), 3195-3216.

[13] Zenk, H., & Akpinar, A. S. (2013, May). PI, PID and fuzzy logic controlled SSSC connected to a power transmission line, voltage control performance comparison. In 4th International Conference on Power Engineering, Energy and Electrical Drives (pp. 1493-1497). IEEE.

[14] Poshtan, M., Singh, B. N., & Rastgoufard, P. (2006, December). A nonlinear control method for SSSC to improve power system stability. In 2006 International Conference on Power Electronic, Drives and Energy Systems (pp. 1-7). IEEE.

[15] Truong, D. N., Tran, Q. C., Tran, P. N., & Thi, M. N. (2018, June). ANFIS damping controller design for SSSC to improve dynamic stability of a grid connected wind power systems. In 2018 International Conference on System Science and Engineering (ICSSE) (pp. 1-5). IEEE.

[16] Falehi, A. D., & Mosallanejad, A. (2016). Neoteric HANFISC–SSSC based on MOPSO technique aimed at oscillation suppression of interconnected multi-source power systems. IET Generation, Transmission & Distribution, 10(7), 1728-1740.

[17] Jolfaei, M. G., Sharaf, A. M., Shariatmadar, S. M., & Poudeh, M. B. (2016). A hybrid PSS–SSSC GA-stabilization scheme for damping power system small signal oscillations. International Journal of Electrical Power & Energy Systems, 75, 337-344.

[18] Kamarposhti, M. A., Colak, I., Iwendi, C., Band, S. S., & Ibeke, E. (2022). Optimal coordination of PSS and SSSC controllers in power system using ant colony optimization algorithm. Journal of circuits, systems and computers, 31(04), 2250060.

[19] Fortes, E. V., Martins, L. F. B., Costa, M. V., Carvalho, L., Macedo, L. H., & Romero, R. (2022). Mayfly Optimization Algorithm Applied to the Design of PSS and SSSC-POD Controllers for Damping Low-Frequency Oscillations in Power Systems. International Transactions on Electrical Energy Systems, 2022(1), 5612334.

[20] Madhusudhan, M., Pradeepa, H., & Jayasankar, V. N. (2023). Grey wolf optimization based fractional order PID controller in SSSC on damping low frequency oscillation in interconnected multi-machine power system. International Journal of Information Technology, 15(4), 2007-2019.

[21] Abdollahi Chirani, A., & Karami, A. (2024). Investigation of the Impact of SSSC-Based FLC on the Stability of Power Systems Connected to Wind Farms. International Transactions on Electrical Energy Systems, 2024(1), 1074029.

[22] Juneja, K. (2022). A fuzzy-controlled differential evolution integrated static synchronous series compensator to enhance power system stability. IETE Journal of Research, 68(6), 4437-4452.

[23] Barik, S. K., & Mohapatra, S. K. (2024). Coordinated control of multi band PSS (MBPSS) with type 2 fuzzy based SSSC controller design for power system stability improvement. Evolutionary Intelligence, 17(3), 1909-1932.

[24] Khadanga, R. K., Das, D., & Panda, S. (2024). Design and Analysis of SSSC-Based Damping Controller: A Novel Modified Zebra Optimization Algorithm Approach. Journal of Electrical and Computer Engineering, 2024(1), 4590764.

[25] Moradi M H, Amiri F. (2022). Improving the stability of the power system based on static synchronous series compensation equipped with robust model predictive control. Journal of Iranian Association of Electrical and Electronics Engineers 19 (4), 291-302

[26] Sahu, P. R., Hota, P. K., & Panda, S. (2019). Modified whale optimization algorithm for coordinated design of fuzzy lead-lag structure-based SSSC controller and power system stabilizer. International Transactions on Electrical Energy Systems, 29(4), 2797.

[27] Amiri, F., & Moradi, M. H. (2021). Angular speed control in a hybrid stepper motor using linear matrix inequality. Computational Intelligence in Electrical

Engineering, 12(3), 33-50..

[28] Amiri, F., & moradi, M. H. (2020). Designing a new robust control method for AC servo motor. Journal of Nonlinear Systems in Electrical Engineering, 7(1), 55-80.

[29] LI, Hongyi; JING, Xingjian; KARIMI, Hamid Reza. Output-feedback-based $ H_ {\infty} $ control for vehicle suspension systems with control delay. IEEE Transactions on Industrial Electronics, 2013, 61.1: 436-446.

[30] Choi, H. D., Ahn, C. K., Lim, M. T., & Song, M. K. (2016). Dynamic output-feedback H∞ control for active half-vehicle suspension systems with time-varying input delay. International Journal of Control, Automation and Systems, 14(1), 59-68.

HOW TO CITE THIS ARTICLE
F. Amiri, S. Sadr, Designing a new robust control method to reduce LFOs in the power system, AUT J. Model. Simul., 57(2) (2025) 139-156.

DOI: 10.22060/miscj.2025.24959.5443